Phenomenological study of unintegrated parton distribution functions in the frameworks of the Kimber-Martin-Ryskin and Martin-Ryskin-Watt approaches

M. Modarres,[1,*] H. Hosseinkhani,[2] and N. Olanj[1]

[1]*Physics Department, University of Tehran, 1439955961 Tehran, Iran*

[2]*Plasma Physics and Fusion Research School, Nuclear Science and Technology Research Institute, 14395-836 Tehran, Iran*

(Received 6 November 2013; published 12 February 2014)

The aim of the present work is to study the phenomenological behavior of unitegrated parton distribution functions (UPDF) by using the Kimber-Martin-Ryskin (KMR) and Martin-Ryskin-Watt (MRW) formalisms. In the first method, the leading order (LO) UPDF of the KMR prescription is extracted, by taking into account the PDF of Martin *et al*., i.e., MSTW2008-LO and MRST99-NLO and. While in the second scheme, the next-to-leading order (NLO) UPDF of the (MRW) procedure is generated through the set of MSTW2008-NLO PDFas the inputs. The different aspects of the UPDF in the two approaches, as well as the input PDF are discussed. Then, the deep inelastic proton structure functions, $F_2(x, Q^2)$, are calculated from the above UPDF in the two schemes, and compared with the data, which are extracted from the ZEUS, NMC, and H1 + ZEUS experimental measurements. In general, it is shown that the calculated structure functions based on the UPDF of two schemes, are consistent to the experimental data, and by a good approximation, they are independent to the input PDF. But the proton structure functions, which are extracted from the KMR prescription, have better agreement to the data with respect to that of MRW. Although the MRW formalism is in more compliance with the Dokshitzer-Bribov-Lipatov-Altarelli-Parisi (DGLAP) evolution equation requisites, but it seems in the KMR case, the angular ordering constraint spreads the UPDF to the whole transverse momentum region, and makes the results to sum up the leading DGLAP and Balitski-Fadin-Kuraev-Lipatov (BFKL) Logarithms. This point is under study by the authors.

DOI: 10.1103/PhysRevD.89.034015 PACS numbers: 12.38.Bx, 13.85.Qk, 13.60.-r

I. INTRODUCTION

The parton distribution functions (PDF), $a(x, \mu^2) = xq(x, \mu^2)$ or $xg(x, \mu^2)$, in which x and μ are the longitudinal momentum fraction and the factorization scale, respectively, are the main theoretical objects in the phenomenological computations, in the high energy particle physics experiments. These PDF are obtained from the global analysis of deep inelastic and related hard scattering data and they satisfy the standard Dokshitzer-Gribov-Lipatov-Altarelli-Parisi (DGLAP) evolution equations [1–4]. The DGLAP equations which are derived by integrating over the parton transverse momentum up to $k_t^2 = \mu^2$. So conventionally, they are called the integrated PDF. Thus the usual PDF are not k_t^2-dependent distributions. The plenty of available experimental data on the various events, such as the exclusive and semi-inclusive processes in the high energy collisions in LHC, indicates the necessity for computation of the k_t-dependent distributions, which are unintegrated over k_t and the are called the unintegrated parton distribution functions (UPDF). The UPDF, $f_a(x, k_t^2, \mu^2)$, are the two-scale dependent functions, i.e., k_t^2 and μ^2, and they satisfy the Ciafaloni-Catani-Fiorani-Marchesini (CCFM) equations [5–9]. Working in this framework is a complicated task. So, in general, the Monte Carlo event generators [10–17] are the main users of these equations. Since there is not a complete quark version of the CCFM formalism, the alternative prescriptions are used for producing the quarks and gluons UPDF. Therefore, to obtain the UPDF, Kimber, Martin and Ryskin (KMR) [18] proposed a different procedure based on the standard DGLAP equations in the LO approximation, along with a modification due to the angular ordering condition, which is the key dynamical property of the CCFM formalism. Later on, Martin, Ryskin and Watt (MRW) extended the KMR approach for the NLO approximation [19], with this aim to improve the exclusive processes. These two procedures, which are reviewed in the Sec. , are the modifications to the standard DGLAP evolution equations and can produce the UPDF by using the PDF as the inputs.

Previously, we have investigated the general behavior and stability of the KMR and MRW prescriptions [20–24]. But here, in order to check the reliability of generated unintegrated parton distributions, we will compare their relative behaviors and use them to calculate the observable, deep inelastic scattering proton structure function

*Corresponding author.
mmodares@ut.ac.ir

$F_2(x, Q^2)$ (see Appendix A). Then the predictions of these two methods for the structure functions, $F_2(x, Q^2)$, are compared to the measurements of NMC [25], ZEUS [26] and H1 + ZEUS [27] experimental data. To proceed this plan, the MRST99 [28] and MSTW2008 [29] set of parton distribution function at the LO and NLO approximations are used as the input PDF. These results as well as our discussions and conclusions are given in the Sec. III.

II. REVIEW OF THE KMR AND THE MRW FORMALISMS

Here, we briefly introduce the explicit forms of UPDF, $f_a(x, k_t^2, \mu^2)$, which have been prescribed by KMR and MRW, respectively, as follows. In the KMR formalism the separation of the real and virtual contributions in the DGLAP evolution chain at the LO level, leads to the following forms for the quark and gluon UPDF:

$$f_q(x, k_t^2, \mu^2) = T_q(k_t, \mu)\frac{\alpha_s(k_t^2)}{2\pi} \times \int_x^{1-\Delta} dz \left[P_{qq}(z)\frac{x}{z}q\left(\frac{x}{z}, k_t^2\right) + P_{qg}(z)\frac{x}{z}g\left(\frac{x}{z}, k_t^2\right)\right], \quad (1)$$

$$f_g(x, k_t^2, \mu^2) = T_g(k_t, \mu)\frac{\alpha_s(k_t^2)}{2\pi} \times \int_x^{1-\Delta} dz \left[\sum_q P_{gq}(z)\frac{x}{z}q\left(\frac{x}{z}, k_t^2\right) + P_{gg}(z)\frac{x}{z}g\left(\frac{x}{z}, k_t^2\right)\right], \quad (2)$$

respectively, where $P_{aa'}(x)$ are the splitting functions and the survival probability factors T_a, are obtained from

$$T_a(k_t, \mu) = \exp\left[-\int_{k_t^2}^{\mu^2} \frac{\alpha_s(k_t'^2)}{2\pi}\frac{dk_t'^2}{k_t'^2} \times \sum_{a'} \int_0^{1-\Delta} dz' P_{a'a}(z')\right]. \quad (3)$$

The cutoff, $\Delta = 1 - z_{\max} = \frac{k_t}{\mu + k_t}$, is determined by imposing the angular ordering condition (AOC) [30,31], which is the consequence of coherent gluon emissions, on the last step of the evolutionary process, to prevent the $z = 1$ singularities in the splitting functions, which arise from the soft gluon emission. As it has been pointed out in Ref. [18], it is worth mentioning again here that in the unified BFKL + DGLAP equation, the scale μ is chosen to be k_t for the DGLAP contribution, which is consistent with the BFKL term (it is independent of μ at LO). So, k_t is the usual choice of scale for α_s in Eqs. (1) and (2). If one chooses something other than k_t for α_s, it would make only a subleading difference [18,32]. The KMR approach has three main characteristics. (a) The unintegrated distributions in the integrals of the evolution ladder, have the form $f_a(x, k_t^2)$, and just at the final step, due to the presence of cutoff, Δ, it becomes μ^2 dependent. (b) The same cutoff is used for all terms in both the quark and gluon evolutions. While using a cutoff, which is obtained from angular ordering condition (AOC) is theoretically apprehensible for gluon parts, but for quarks, it can be understood only phenomenologically. (c) The existence of the cutoff at the upper limit of the integrals, makes the distributions to spread smoothly to the region in which $k_t > \mu$, a characteristic of the small x physics, which is principally governed by the Balitski-Fadin-Kuraev-Lipatov (BFKL) evolution [33–37]. The latter feature of the KMR, leads to the UPDF with the behavior very similar to the unified BFKL + DGLAP formalism [18]. These kinds of UPDF have been widely used for phenomenological calculations related to the k_t dependent distributions (see [38–49] and also [21] and the references therein). In the MRW formalism, the same separation of real and virtual contributions to the DGLAP evolution is done, but the procedure is at the NLO level. The general forms of their UPDF are

$$f_a^{\rm NLO}(x, k_t^2, \mu^2) = \int_x^1 dz T_a(k^2, \mu^2)\frac{\alpha_s(k^2)}{2\pi} \times \sum_{b=q,g} P_{ab}^{(0+1)}(z) b^{\rm NLO}\left(\frac{x}{z}, k^2\right) \times \Theta(\mu^2 - k^2), \quad (4)$$

where

$$P_{ab}^{(0+1)}(z) = P_{ab}^{(0)}(z) + \frac{\alpha_s}{2\pi}P_{ab}^{(1)}(z), \qquad k^2 = \frac{k_t^2}{1-z}. \quad (5)$$

In Eqs. (4) and (5) the $P_{ab}^{(0)}$ and the $P_{ab}^{(1)}$ denote the LO and the NLO contributions of splitting functions, respectively. It is obvious from Eq. (4) that, in the MRW formalism, the UPDF are defined such that, to ensure $k^2 < \mu^2$. Also, the survival probability factors, T_a, are obtained as follows:

$$T_a(k^2, \mu^2) = \exp\left(-\int_{k^2}^{\mu^2} \frac{\alpha_s(\kappa^2)}{2\pi}\frac{d\kappa^2}{\kappa^2} \times \sum_{b=q,g} \int_0^1 d\zeta\zeta P_{ba}^{(0+1)}(\zeta)\right), \quad (6)$$

where $P_{ab}^{(i)}$ (which is singular in the $z \to 1$) is given in Ref. [50]. Therefore the MRW formalism shows the first characteristics of the KMR approach, but not the second,

and (obviously) the third ones. Consequently the MRW mechanism is more faithful to the DGLAP prerequisites.

MRW have demonstrated that the sufficient accuracy can be obtained by keeping only the LO splitting functions, together with the NLO integrated parton densities. So, by considering angular ordering, we can use $P^{(0)}$ instead of $P^{(0+1)}$. As it is mentioned above, unlike the KMR formalism, where the angular ordering is imposed in the all of the terms of the Eqs. (1) and (2), in the MRW formalism, the angular ordering is imposed by the terms in which the splitting functions are singular, i.e., the terms which include P_{qq} and P_{gg}.

III. RESULTS, DISCUSSIONS AND CONCLUSIONS

As it was described in the Sec. II, the KMR and MRW formalisms operate as the UPDF generating mechanisms, with the input PDF. In order to make the comparison more clear, the typical inputs, the gluon and up quark PDF at scale $Q^2 = 27$ GeV^2, by using the MRST99-NLO [28] (full curves), MSTW2008-LO [29] (dash curves) and MSTW2008-NLO [29] (dot curves), are plotted in Fig. 1. The well known behavior of these integrated PDF has been discussed in detail in the related Refs. [28,29]. In particular: The sizable NLO contributions (especially for the gluons PDF) at very low x regions and the similarity of MRST99-NLO and MSTW2008-NLO data, for different values of x are clearly seen. In Fig. 2, the general behaviors of gluons and up quarks UPDF (f_g and f_u) versus x, for the KMR and MRW approaches are shown. The typical factorization scales are $\mu^2 = 27$ and 100 GeV^2, for the left and right panels, respectively. The results are obtained at $k_t^2 = 0.4\mu^2$ and $0.9\mu^2$. For better comparison of two prescriptions, i.e., KMR and MRW, we have used the same inputs, i.e., MSTW2008-NLO PDF. At $k_t^2 = 0.4\mu^2$ the output UPDF are similar, but by increasing the transverse momentum to $k_t^2 = 0.9\mu^2$, there are a sizable decrease in the MRW-UPDF (dash curves), and they become different from the KMR-UPDF (solid curves). On the other hand, by increasing the factorization scale from $\mu^2 = 27$ to 100 GeV^2, the differences slowly rise due to the growing of the KMR-UPDF. The values of these differences are more sensitive to the variation of the k_t, than the PDF scales μ^2. It is clear from large discrepancies due to changing the k_t^2 from $0.4\,\mu^2$ to $0.9\,\mu^2$ along each column in Fig. 2, (for example, 13.5 GeV^2 for $\mu^2 = 27$ GeV^2), which can be compared with the smaller discrepancies for the change in the factorization scale, μ^2, from 27 to 100 GeV^2 (73 GeV^2), in each row. These effects are more prominent in the case of up quarks. The appearance of these features has roots in the characteristics of the KMR and MRW schemes. As it was stated in the Sec. II, applying the angular ordering constraint (AOC) on all terms in the KMR equations, leads to a behavior very similar to the unified BFKL + DGLAP approach [18], which in turn brings, different behaviors from the MRW, that is more DGLAP

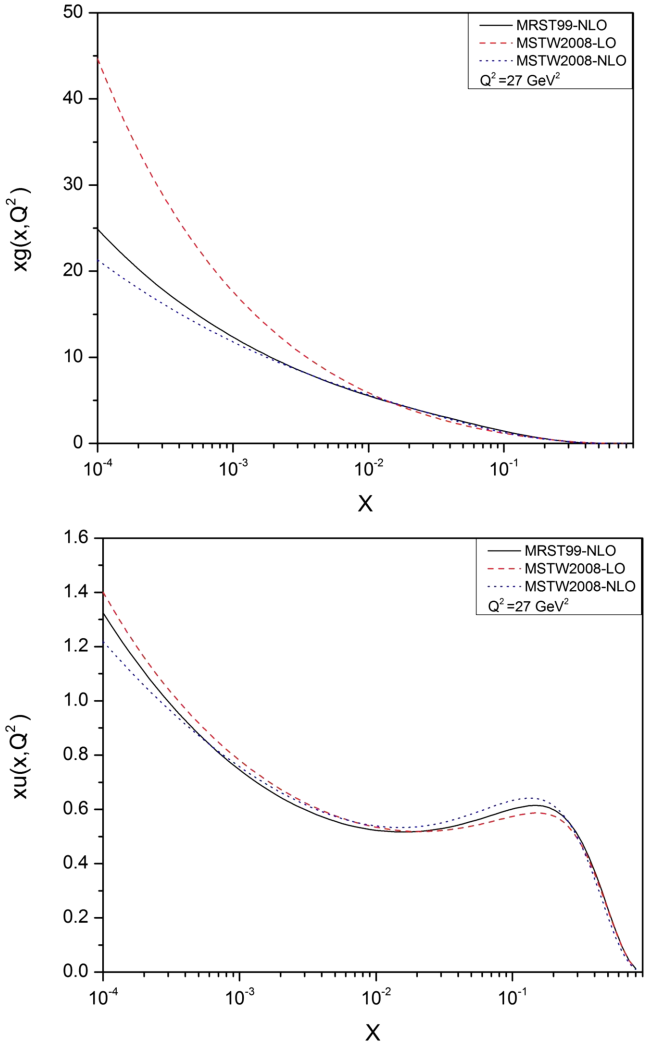

FIG. 1 (color online). The integrated gluon and up quark distribution function (see the text for detail).

like approach, especially at lower values of x. In all of the diagrams of Fig. 2, the discrepancies grow up with reduction of x. Therefore the growth of k_t and lowering x, which are characteristics of the very high energy and k_t-factorization region, cause more differences, in comparison to the variation of the factorization scale μ^2, which is a common feature of both prescriptions, inherited from the DGLAP evolution. On the other hand, although the increase of the scale μ^2 causes similar effects in the input PDF for both frameworks, but in the KMR equations, because of the dependence of upper limit of z integration on the scale μ (i.e., $z_{\max} = \frac{\mu}{\mu + k_t}$), by growing μ, the upper limit $z_{\max}$ increases, which in turn leads to additional rise in the output UPDF.

The difference between these two prescriptions is more distinguishable in the quark parts, where MRW is more restricted to the collinear factorization requirements. The above features can be seen again in Fig. 3, where for comparing the UPDF at LO and NLO approximation, the

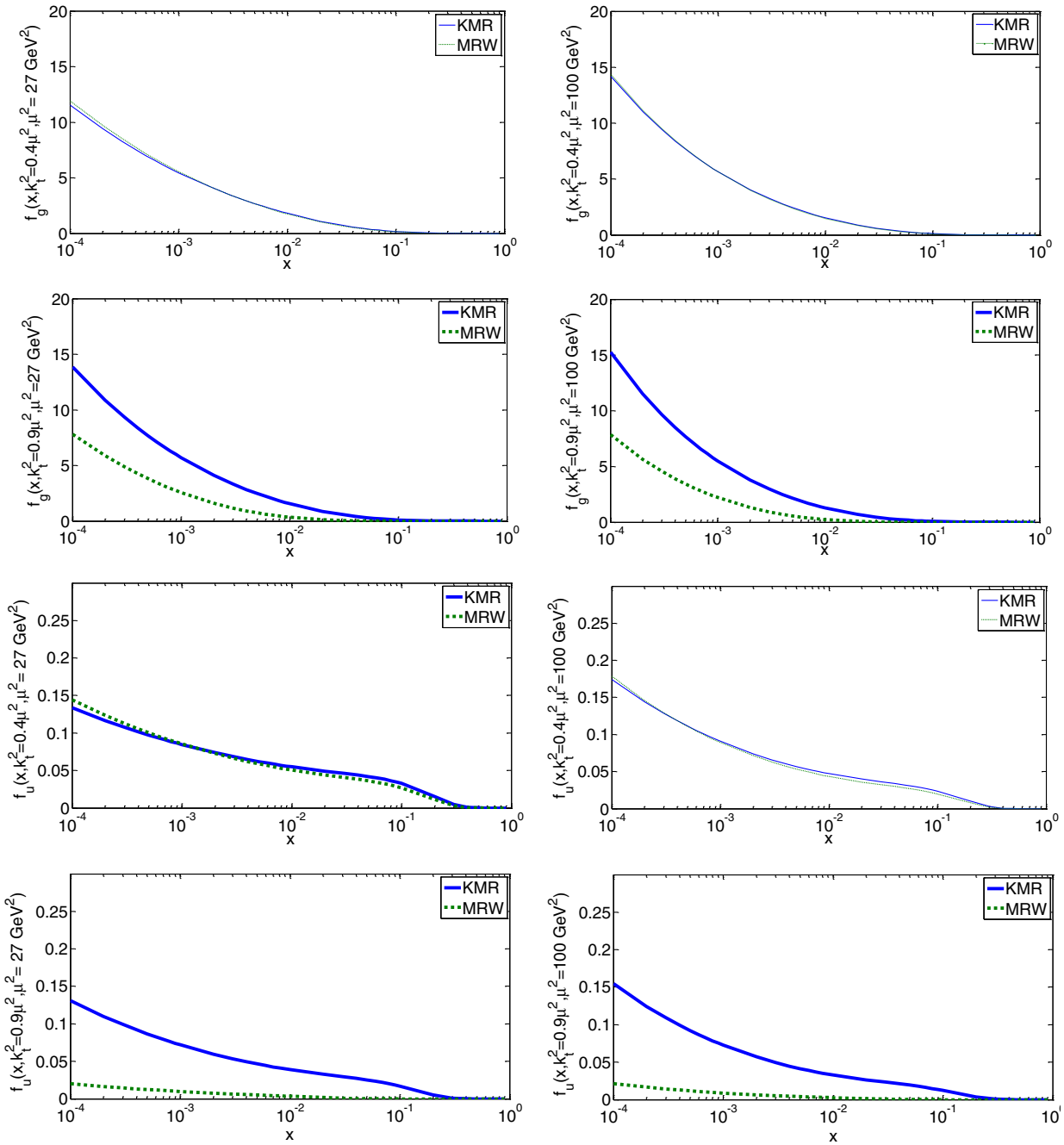

FIG. 2 (color online). The unintegrated gluon and up quark distribution function versus x using MSTW2008-NLO PDF as the inputs.

LO and NLO PDF are used as the appropriate inputs for the KMR and MRW formalisms, respectively. In addition to above characteristics, more discrepancies appear at lower values of x, which are a heritage of the same behavior of parent PDF (see Fig. 1). It is interesting that at lower values of k_t, where the situation is closer to the collinear state, the differences decrease compares to the parent PDF. Previously we have studied in details the general behavior of these kinds of UPDF in Refs. [20–24]. In these works, in each type of above approaches, the stability of the output UPDF versus the variation of input PDF has been tested. In Fig. 3, by reducing k_t, two types of the UPDF approach to a unique distribution and the PDF discrepancies are suppressed in the outputs.

In Fig. 4, the UPDF are plotted versus k_t^2 at typical values of $x = 0.1$, 0.01, and 0.001 and the factorization scale $\mu^2 = 100\ \mathrm{GeV}^2$. The above features are again observed in Fig. 4, i.e., such as the remarkable distinctions at high k_t^2. Here the input distributions are the same, i.e., MSTW2008-NLO. At large x, the difference between the dynamical scales in the evolution chain, i.e., k_t^2 in the KMR and $k^2 = \frac{k_t^2}{1-z}$ in the MRW, become important [19,20], that in

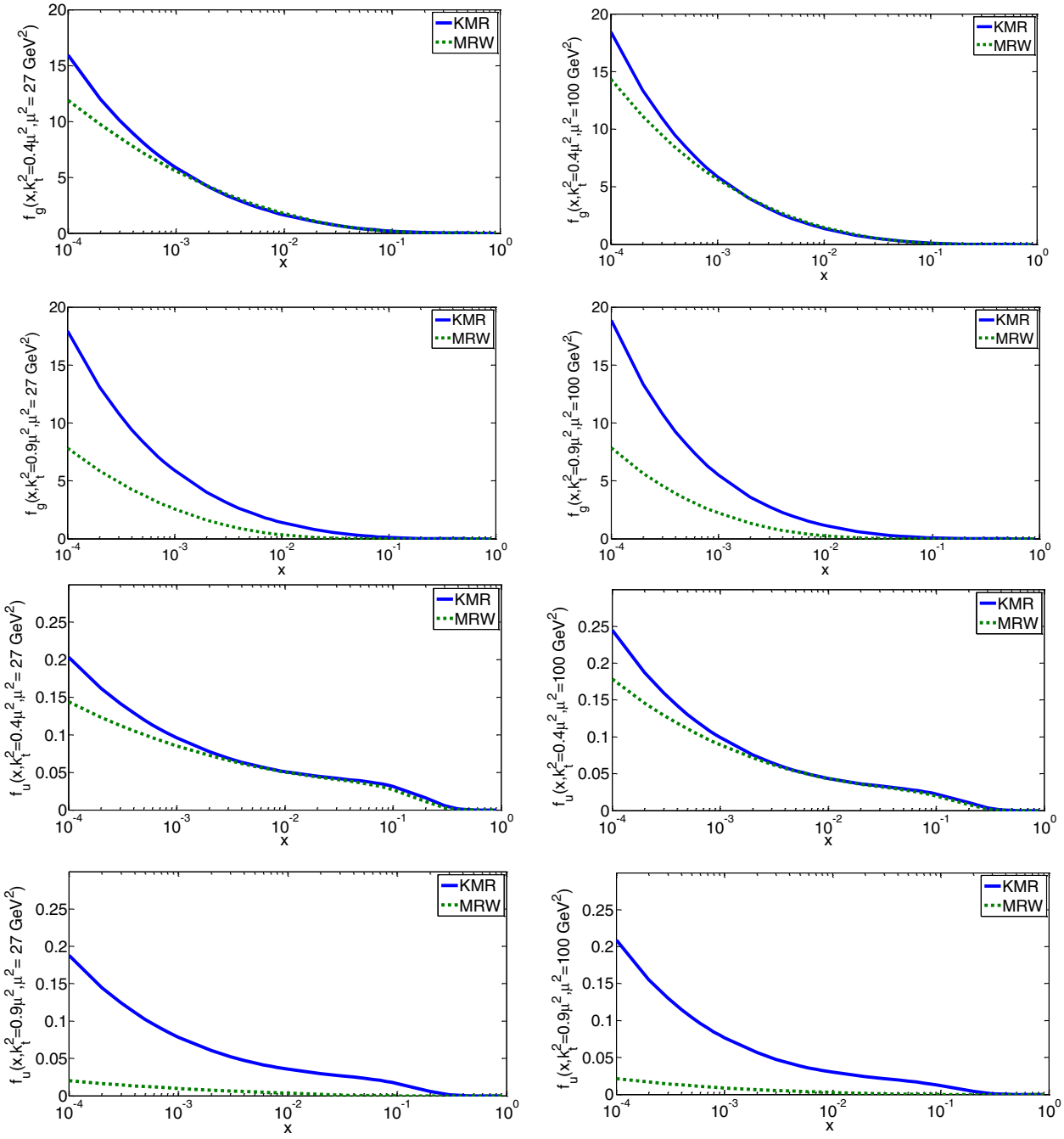

FIG. 3 (color online). The unintegrated gluon and up quark distribution function versus x with the KMR [18] (MRW [19]) prescriptions by using the MSTW2008-LO PDF (MSTW2008-NLO PDF) as the inputs.

turn affects the domain of integration in the PDF and particularly for $\alpha_s(k^2)$ (see the Eqs. (4) and (6)), which leads to the relative reduction of MRW-UPDF, especially at lower k_t^2, where the relative variation raises. At lower x, the above differences are suppressed, but the presence of cutoff Δ in the KMR Eqs. (1–3), causes the relative decrease in the KMR-UPDF. This behavior is more noticeable in the quark UPDF, where the different application of AOC is specified. The AOC (in the form of Δ) is applied to all terms in the KMR, but only to the singular terms in the MRW. Because of the convolution forms of evolution equations and the larger amplitude of input gluon PDF, it is natural that both sets of the gluon UPDF (f_g) become very similar. While in the case of quarks, the role of singular splitting function P_{qq} suppressed by the lower values of the input quark PDF, and the role of nonsingular term, such as $P_{qg} \times g$ in Eq. (4), becomes more prominent. One should notice that, the KMR prescription is a LO scheme and more compatible inputs are LO PDF. This is what has been plotted in Fig. 5, where like Fig. 3, the LO

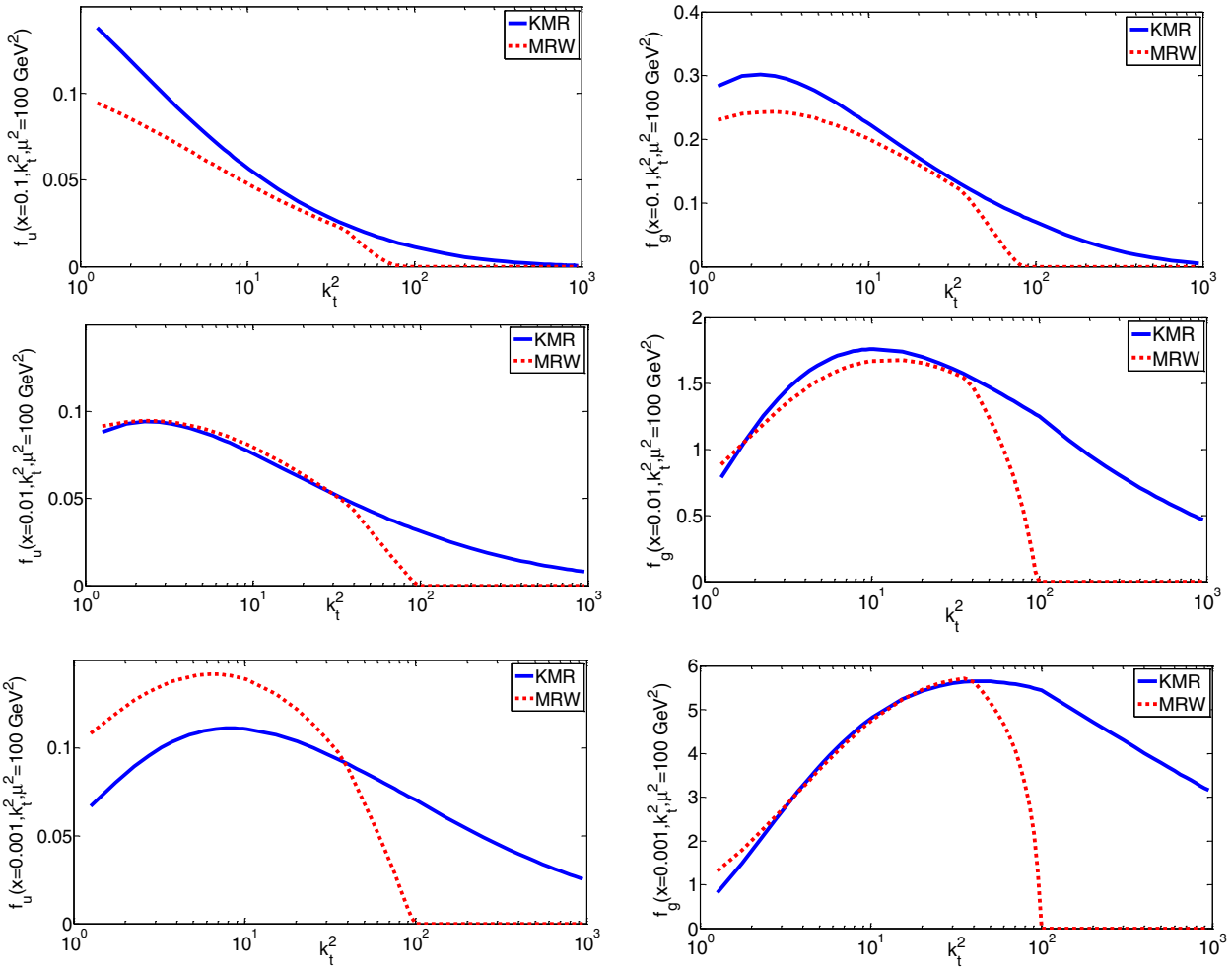

FIG. 4 (color online). The unintegrated gluon and up quark distribution function versus k_t^2 using MSTW2008-NLO PDF as the inputs for the KMR [18] and MRW [19] prescriptions.

and NLO PDF are used in the KMR and MRW frameworks, respectively. Unlike the former behavior, here both of the UPDF sets, approach to the unique outputs. The exception is for $x = 0.1$ i.e., at large x, where the distinctions between k_t^2 and k^2 is important, as it was discussed previously.

For more precise investigation, it is useful to use these UPDF in the phenomenological calculations of high energy observable, and analyze their results in the exclusive processes. Here we proceed this study, by computing the inclusive observable $F_2(x, Q^2)$ with both types of the calculated UPDF, via the k_t-factorization framework, as its input. The calculation procedure is introduced briefly in the Appendix A [18]. The resulting structure functions, $F_2(x, Q^2)$, versus x are plotted in Fig. 6 and compared with the data from the NMC [25], ZEUS [26] and H1 + ZEUS [27] measurements at scales $Q^2 = 27$, 90, and 250 GeV^2. The UPDF applied for this procedure are the KMR and MRW at the LO and NLO, respectively by using the MSTW2008 set of PDF at the LO and NLO as inputs. As it is expected, the main contribution to the $F_2(x, Q^2)$ at low x, comes from the gluons $(f_g(x, k_t^2, \mu^2))$, while at large x, it belongs to the quarks $(f_q(x, k_t^2, \mu^2))$. For the KMR approach, the results are also generated by using the MRST99-NLO set of partons that is used in Ref. [18]. As it has been demonstrated, the two sets of $F_2(x, Q^2)$ graphs are obtained by using the KMR distributions. The small differences are due to the variations in the input PDF, i.e., MRST99-NLO and MSTW2008-LO. As it was shown in Refs. [21–24], the KMR formalism suppresses the discrepancies between the inputs PDF, in which the presence of cutoff $\Delta = \frac{k_t}{\mu + k_t}$ has the key role. This property leads the outputs UPDF which are more similar. As a result, the UPDF generated via applying two different inputs PDF have less discrepancies and in turn, the $F_2(x, Q^2)$ values are very close to each other. Although, the plots become different at smaller values of x, but it happens at very lower rate than the PDF themselves. For obtaining the values of $F_2(x, Q^2)$, by using the MRW distributions, because of the heavier amount of computations, the typical points are considered. On the other hand, the computation time increases by raising the scale Q^2. The effects of former

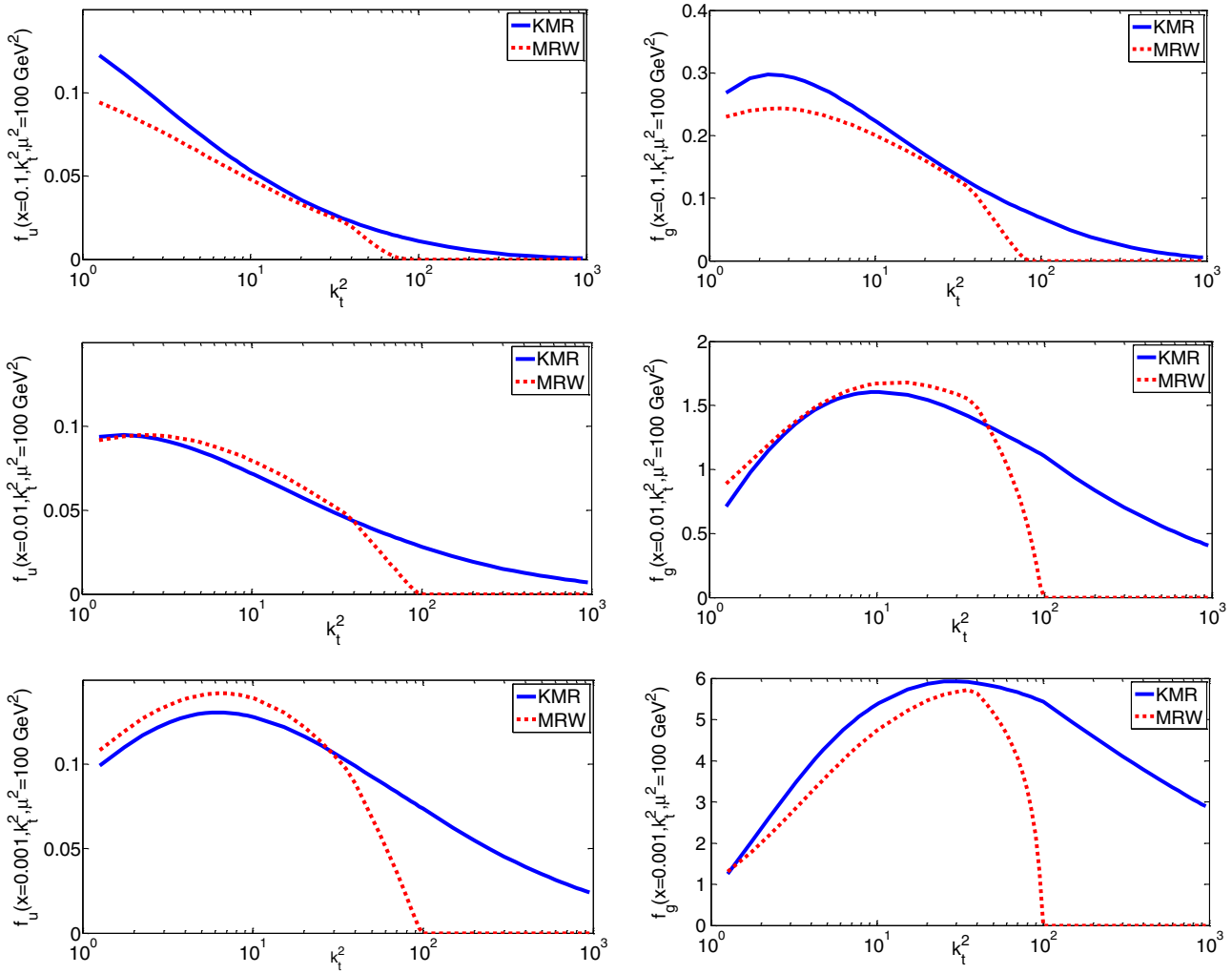

FIG. 5 (color online). The unintegrated gluon and up quark distribution function versus k_t^2 with the KMR [18] (MRW [19]) prescriptions by using the MSTW2008-LO PDF (MSTW2008-NLO PDF) as the inputs.

discussed features of the UPDF, are appeared in the resulted $F_2(x, Q^2)$ (see Fig. 6). The smaller values of MRW UPDF in Figs. 3 and 5, leads to the lower estimate for $F_2(x, Q^2)$. As a general behavior, the values of $F_2(x, Q^2)$ are relatively in good agreement with the experimental data, although the KMR results are more consistent, especially at higher Q^2 scales. The better agreement on the KMR approach can be interpreted as a consequence of its continuation to the $k_t > \mu$ domain, which is far from the standard DGLAP scope, i.e., a behavior that has roots in applying the AOC and is similar to a BFKL type effect [18]. We have to emphasize that this is not a final justification between the KMR and MRW approaches. For example, the deviations from the experimental data of $F_2(x, Q^2)$ can lead to refitting the data in order to make the output UPDF and the final extracted $F_2(x, Q^2)$ (in the k_t-factorization scheme) more consistent.

It should be noted that there are two different roles in the single-scale distributions for the description of data in the inclusive observable. The first role is the traditional one, where the integrated parton distribution functions are fitted directly to the data in the framework of collinear factorization, for example, see [29] and [28]. The second role is demonstrated in the KMR and MRW approaches, where the single-scale functions are used as an input to the last-step procedure, see for example Eq. (1). In this case, the single-scale functions should be determined by a global fit to the same data using the k_t-factorization framework. Similar to Ref. [18], we have produced the unintegrated parton distribution functions in the frameworks of KMR and MRW approaches, (which is based on the AOC constraint), by using the traditional integrated parton distribution functions as the input to the last step of the evolution. As it has been explained in Ref. [51], this treatment is adequate for initial investigations and descriptions of exclusive processes. Although the traditional PDF have been fitted via the collinear factorization framework to the deep inelastic scattering data, Fig. 6 shows that the $F_2(x, Q^2)$ which is calculated from these unintegrated parton distribution functions give an adequate description

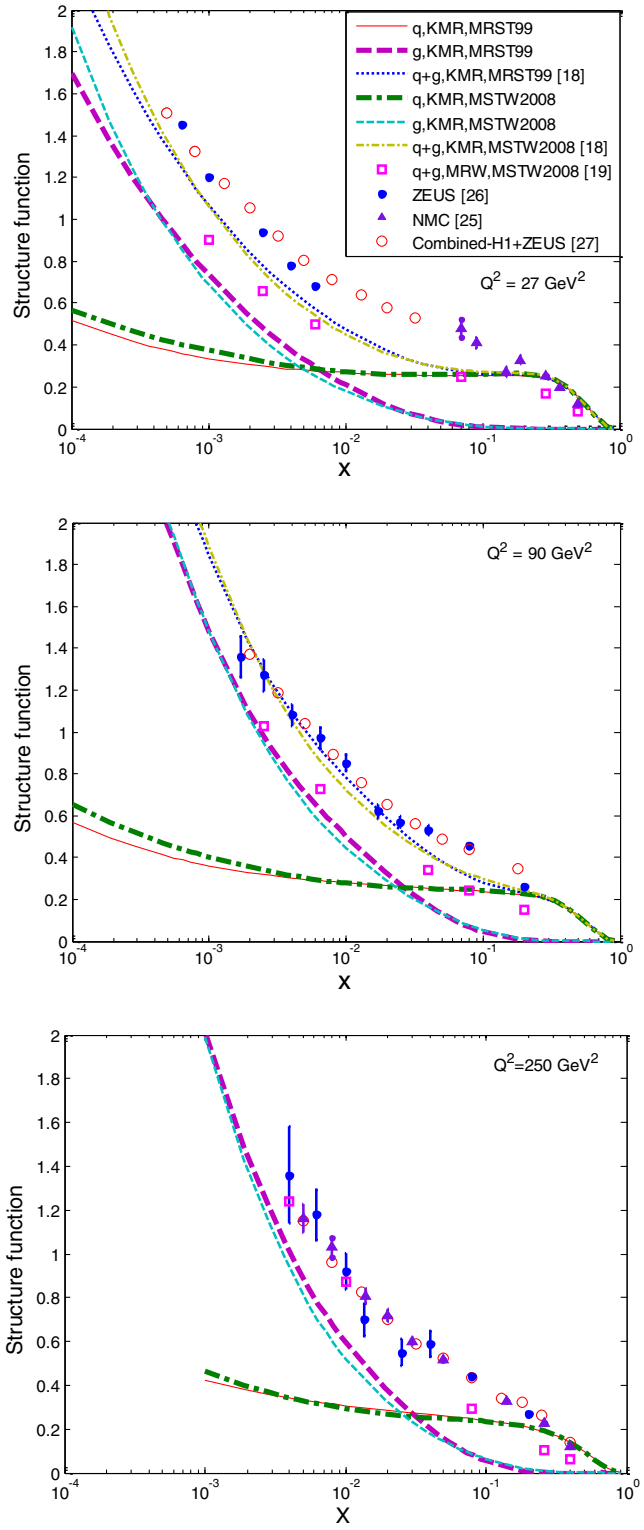

FIG. 6 (color online). The deep inelastic proton structure functions $F_2(x, Q^2)$ with the KMR [18] (MRW [19]) prescriptions by using the MRST99-NLO [28] and the MSTW2008-LO (MSTW2008-NL0) [29] as the inputs. Note that q (g ($q + g$)) is the contribution of unintegrated quarks to $F_2(x, Q^2)$ (the contribution of unintegrated gluon to $F_2(x, Q^2)$ (the structure function $F_2(x, Q^2)$ which is the sum of q and g)).

of the data, especially at high Q^2. Therefore, as it was stated before, the obtained UPDF may be used to evaluate the exclusive processes, a work which is in progress also by the present authors. So, we would expect that the small discrepancy between the k_t-factorization prediction of $F_2(x, Q_2)$ and the experimental data can be eliminated by using the PDF which have been fitted to the same data using the k_t-factorization framework. In this case as it has been mentioned in Refs. [18,52] the relation between the PDF and UPDF will be exactly satisfied, i.e.,

$$a(x, \mu^2) = \int^{\mu^2} \frac{dk_t^2}{k_t^2} f_a(x, k_t^2, \mu^2).$$

On the other hand, one can follow the angular-ordered CCFM equation to satisfy the above equation [52], which leads to the incomplete angular ordering of the BFKL contribution (for example, see the Sec. VI of Ref. [18]).

In conclusion, the phenomenological investigation of Kimber-Martin-Ryskin and Martin-Ryskin-Watt unintegrated parton distribution functions as well as the phenomenological study of the proton deep inelastic structure functions $F_2(x, Q^2)$ was performed in this work. In the first method, the leading order UPDF of the KMR prescriptions were applied, by taking into account the PDF of Martin *et al.*, i.e., MSTW2008-LO and MRST99-NLO. While in the second scheme, the next-to-leading order UPDF of the Martin-Ryskin-Watt procedures were used with the PDF of MSTW2008-NLO as the inputs. The different aspects of the UPDF in the two approaches as well as the input PDF were discussed. Then, the deep inelastic proton structure functions, $F_2(x, Q^2)$ were calculated from the unintegrated parton distribution functions in the two schemes, and compared with the data which were extracted from the ZEUS, NMC and H1+ZEUS experimental measurements. In general, it was shown that the calculated structure functions based on the UPDF were consistent with the experimental data, and with good approximation, they were independent of the input PDF. But the proton structure functions which were extracted from the KMR prescription have better agreement to the data with respect to that of MRW. Although the MRW formalism is in more compliance with the Dokshitzer-Gribov-Lipatov-Altarelli-Parisi (DGLAP) evolution equations requisites, but in the KMR case, the angular ordering constraint spreads the UPDF to whole transverse momentum region and it seems that the KMR formalism makes the results to sum up the leading DGLAP and Balitski-Fadin-Kuraev-Lipatov (BFKL) logarithms. The longitudinal structure function, $F_L(x, Q^2)$, can a be also calculated by using the same formalisms and compared with those give in Refs. [53–55], and the HERA data [27]. With this comparison the UPDF presented in this work can be better evaluated for the future calculations.

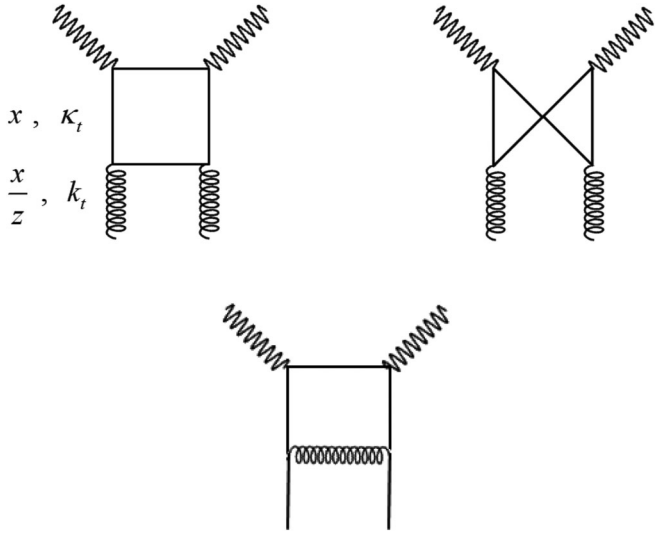

FIG. 7. The diagrams contributing in the calculation of the structure functions $F_2(x,Q^2)$, which comes from the $g \to q\bar{q}$ and $q \to qg$.

ACKNOWLEDGMENTS

MM would like to acknowledge the Research Council of University of Tehran and Institute for Research and Planning in Higher Education for the grants provided for him. The authors would like to thank Ms. F. Nasrolahinasab for her contribution at the beginning of this work.

APPENDIX CALCULATION OF $F_2(x,Q^2)$ IN THE k_t-FACTORIZATION

Here we briefly describe the different steps for calculations of the structure function $F_2(x,Q^2)$, from the unintegrated parton distributions [18], in which the unintegrated gluons and quarks distributions are equally treated as the inputs to $F_2(x,Q^2)$. The unintegrated gluons and quarks contributions to $F_2(x,Q^2)$ come from the $g \to q\bar{q}$ and $q \to qg$, respectively. The relevant diagrams are those shown in Fig. 7. As it was noted before, the gluons in the proton can only contribute to $F_2(x,Q^2)$ via an intermediate quark, so one should calculate $F_2(x,Q^2)$ in the k_t-factorization approach by using the gluons and quarks UPDF. There are six diagrams corresponding to the subprocess $g \to q\bar{q}$ and $q \to qg$, (see Fig. 6 of Ref. [56]). Similar to Ref. [56], a physical gauge for the gluon, i.e., $A^\mu q'_\mu = 0$ ($q^{\text{prime}} = q + xp$), should be fixed such that the splitting kernels are obtained only from the ladder-type diagrams. Therefore, the diagrams where a gluon is *radiated from the final quark line* (comes from the subprocess $q \to qg$) are strongly suppressed in this gauge, due to one or more of the propagators, which have the very large virtualities. So, the diagrams of Fig. 7 are the only contributions which should be included in the proton structure function. The crossed box diagram which comes from the subprocess $g \to q\bar{q}$ is included, although it gives only a relatively small contribution to the cross section.

These contributions may be written in the k_t factorization form, by using the unintegrated gluon distributions $f_g(\frac{x}{z}, k_t^2, \mu^2)$ as follows [57–60]:

$$F_2(x,Q^2) = \int_x^1 \frac{dz}{z} \int \frac{dk_t^2}{k_t^2} f\left(\frac{x}{z}, k_t^2\right) S_{\text{box}}(z, k_t^2, Q^2), \quad \text{(A1)}$$

where the part of S_{box}, which contains the quark box and crossed box approximations to the photon-gluon subprocess, is evaluated in Refs. [53,54,61], which leads to the $g \to q\bar{q}$ structure function:

$$F_2^{g\to q\bar{q}}(x,Q^2) = \sum_q e_q^2 \frac{Q^2}{4\pi} \int \frac{dk_t^2}{k_t^4} \int_0^1 d\beta \int d^2\kappa_t \alpha_s(\mu^2) f_g\left(\frac{x}{z}, k_t^2, \mu^2\right) \Theta\left(1 - \frac{x}{z}\right)$$
$$\times \left\{ [\beta^2 + (1-\beta^2)] \left(\frac{\kappa_t}{D_1} - \frac{(\kappa_t - k_t)}{D_2}\right)^2 + [m_q^2 + 4Q^2\beta^2(1-\beta)^2] \left(\frac{1}{D_1} - \frac{1}{D_2}\right)^2 \right\}. \quad \text{(A2)}$$

In the above equation, in which the graphical representations of k_t and κ_t have been introduced in Fig. 7, the variable β is defined as the light-cone fraction of the photon momentum carried by the internal quark [18]. Also, the denominator factors are

$$D_1 = \kappa_t^2 + \beta(1-\beta)Q^2 + m_q^2,$$
$$D_2 = (\kappa_t - k_t)^2 + \beta(1-\beta)Q^2 + m_q^2, \quad \text{(A3)}$$

and

$$\frac{1}{z} = 1 + \frac{\kappa_t^2 + m_q^2}{(1-\beta)Q^2} + \frac{k_t^2 + \kappa_t^2 - 2\kappa_t.k_t + m_q^2}{\beta Q^2}. \quad \text{(A4)}$$

As in Ref. [53], the scale μ controls the unintegrated gluon and the QCD coupling constant α_s is chosen as follows,

$$\mu^2 = k_t^2 + \kappa_t^2 + m_q^2. \quad \text{(A5)}$$

The charm quark mass is taken to be $m_c = 1.4$ GeV, and u, d and s quarks masses are neglected. As in Ref. [32], to save the computation time, we also use the same

approximation, i.e., the representative "average" value for ϕ, $\langle\phi\rangle = \frac{\pi}{4}$. The unintegrated gluons distributions are not defined for $k_t < k_0$, i.e., the nonperturbative region. So, according to Ref. [54], k_0 is chosen to be about 1 GeV, which is around the charm mass in the present calculation, as it should be. Then, the contribution of the nonperturbative region for the gluons is approximated, as follows,

$$\int_0^{k_0^2} \frac{dk_t^2}{k_t^2} f_g(x,k_t^2,\mu^2)\left[\frac{\text{remainder of equation (A2)}}{k_t^2}\right] \simeq xg(x,k_0^2)T_g(k_0,\mu)[]_{k_t=a}, \tag{A6}$$

where a is a suitable value of k_t between 0 and k_0, which its value is not important to the nonperturbative contribution.

The contributions of unintegrated quarks to $F_2(x,Q^2)$ come from an "initial" quark with Bjorken scale $\frac{x}{z}$ and the perturbative transverse momentum $k_t > k_0$, which split to a radiated gluon and a quark with Bjorken scale x and transverse momentum κ_t. This "final" quark interacts with the photon and contributes to the $F_2(x,Q^2)$, as follows,

$$F_{2\text{perturbative}}^{\text{quark}\to\text{quark}}(x,Q^2) = \sum_{q=u,d,s,c} e_q^2 \int_{k_0^2}^{Q^2} \frac{d\kappa_t^2}{\kappa_t^2}\frac{\alpha_s(\kappa_t^2)}{2\pi}\int_{k_0^2}^{\kappa_t^2}\frac{dk_t^2}{k_t^2}\int_x^{\frac{Q}{(Q+k_t)}} dz\left[f_q\left(\frac{x}{z},k_t^2,Q^2\right)+f_{\bar{q}}\left(\frac{x}{z},k_t^2,Q^2\right)\right]P_{qq}(z). \tag{A7}$$

The contribution of the nonperturbative region is also calculated according to Ref. [18]:

$$F_2{}^{q(\text{nonperturbative})}(x,Q^2) = \sum_q e_q^2(xq(x,k_0^2)+x\bar{q}(x,k_0^2))T_q(k_0,Q). \tag{A8}$$

Finally, the structure function $F_2(x,Q^2)$ is given by the sum of the gluon contributions, the Eqs. (A2) and (A6), and the quark contributions, the Eqs. (A7) and (A8).

[1] V. N. Gribov and L. N. Lipatov, Yad. Fiz. **15**, 781 (1972).
[2] L. N. Lipatov, Sov. J. Nucl. Phys. **20**, 94 (1975).
[3] G. Altarelli and G. Parisi, Nucl. Phys. **B126**, 298 (1977).
[4] Y. L. Dokshitzer, Sov. Phys. JETP **46**, 641 (1977).
[5] M. Ciafaloni, Nucl. Phys. **B296**, 49 (1988).
[6] S. Catani, F. Fiorani, and G. Marchesini, Phys. Lett. B **234**, 339 (1990).
[7] S. Catani, F. Fiorani, and G. Marchesini, Nucl. Phys. **B336**, 18 (1990).
[8] G. Marchesini, *Proceedings of the Workshop QCD at 200 TeV, Erice, Italy*, edited by L. Cifarelli and Yu. L. Dokshitzer (Plenum, New York, 1992), p. 183.
[9] G. Marchesini, Nucl. Phys. **B445** 49 (1995).
[10] H. Kharraziha and L. Lönnblad, J. High Energy Phys. 03 (**1998**) 006.
[11] G. Marchesini and B. Webber, Nucl. Phys. **B349**, 617 (1991).
[12] G. Marchesini and B. Webber, Nucl. Phys. **B386**, 215 (1992).
[13] H. Jung, Nucl. Phys. **B79**, 429 (1999).
[14] H. Jung and G. P. Salam, Eur. Phys. J. C, **19**, 351 (2001).
[15] H. Jung, J. Phys. G **28**, 971 (2002).
[16] H. Jung *et al.*, Eur. Phys. J. C **70**, 1237 (2010).
[17] H. Jung, M. Kraemer, A. V. Lipatov, and N. P. Zotov, J. High Energy Phys. 01 (**2011**) 085.
[18] M. A. Kimber, A. D. Martin, and M. G. Ryskin, Phys. Rev. D **63**, 114027 (2001).
[19] A. D. Martin, M. G. Ryskin, and G. Watt, Eur. Phys. J. C **66**, 163 (2010).
[20] M. Modarres, H. Hosseinkhani, and N. Olanj, Nucl. Phys. **A902**, 21 (2013).
[21] M. Modarres and H. Hosseinkhani, Few-Body Syst., **47**, 237 (2010).
[22] M. Modarres and H. Hosseinkhani, Nucl. Phys. **A815**, 40 (2009).
[23] H. Hosseinkhani and M. Modarres, Phys. Lett. B **694**, 355 (2011).
[24] H. Hosseinkhani and M. Modarres, Phys. Lett. B **708** 75 (2012).
[25] NMC: Arneodo *et al.*, Nucl. Phys. **B483**, 3 (1997).
[26] ZEUS: Derrick *et al.*, Z. Phys. C **72**, 399 (1996).
[27] H1 and ZEUS Collaborations, J. High Energy Phys. 01 (**2010**) 109.
[28] A. D. Martin, R. G. Roberts, W. J. Stirling, and R. S. Thorne, Eur. Phys. J. C **14**, 133 (2000).
[29] A. D. Martin, W. J. Stirling, R. S. Thorne, and G. Watt, Eur. Phys. J. C **63**, 189 (2009).
[30] G. Marchesini and B. R. Webber, Nucl. Phys. **B310**, 461 (1988).
[31] Yu. L. Dokshitzer, V. A. Khoze, S. I. Troyan, and A. H. Mueller, Rev. Mod. Phys. **60**, 373 (1988).
[32] M. A. Kimber, Ph. D. Thesis, University of Durham, United Kingdom, 2001.
[33] V. S. Fadin, E. A. Kuraev, and L. N. Lipatov, Phys. Lett. **60B**, 50 (1975).
[34] L. N. Lipatov, Sov. J. Nucl. Phys. **23**, 642 (1976).

[35] E. A. Kuraev, L. N. Lipatov and V. S. Fadin, Sov. Phys. JETP **44**, 45 (1976).
[36] E. A. Kuraev, L. N. Lipatov, and V. S. Fadin, Sov. Phys. JETP **45**, 199 (1977).
[37] Ya.Ya. Balitsky and L. N. Lipatov, Sov. J. Nucl. Phys. **28**, 822 (1978).
[38] V. A. Saleev, Phys. Rev. D, **80**, 114016 (2009).
[39] A. V. Lipatov and N. P. Zotov, Phys. Rev. D **81**, 094027 (2010).
[40] S. P. Baranov, A. V. Lipatov, and N. P. Zotov, Phys. Rev. D **81**, 094034 (2010).
[41] B. A. Kniehl, V. A. Saleev, and A. V. Shipilova, Phys. Rev. D **81**, 094010 (2010).
[42] H. Jung, M. Kraemer, A. V. Lipatov, and N. P. Zotov, J. High Energy Phys. 01 (**2011**) 085.
[43] S. P. Baranov, A. V. Lipatov, and N. P. Zotov, Eur. Phys. J. C **71**, 1631 (2011).
[44] A. V. Lipatov, M. A. Malyshev, and N. P. Zotov, Phys. Lett. B **699**, 93 (2011).
[45] H. Jung, M. Kraemer, A. V. Lipatov, and N. P. Zotov, arXiv:1105.5071.
[46] H. Jung, M. Kraemer, A. V. Lipatov, and N. P. Zotov, Phys. Rev. D **85**, 034035 (2012).
[47] A. V. Lipatov and N. P. Zotov, Phys. Lett. B **704**, 189 (2011).
[48] B. A. Kniehl, V. A. Saleev, A. V. Shipilova, and E. V. Yatsenko, Phys. Rev. D **84**, 074017 (2011).
[49] H. Jung, M. Kraemer, A. V. Lipatov, and N. P. Zotov, Phys. Rev. D **85**, 034035 (2012).
[50] W. Furmanski and R. Petronzio, Phys. Lett. **97B**, 437 (1980).
[51] G. Watt, A. D. Martin, and M. G. Ryskin, Phys. Rev. D **70** 014012 (2004).
[52] M. A. Kimber, J. Kwiecinski, A. D. Martin, and A. M. Stasto, Phys. Rev. D **62**, 094006 (2000).
[53] J. Kwiecinski, A. D. Martin, and A. M. Stasto, Phys. Rev. D, **56** 3991 (1997).
[54] A. J. Askew, J. Kwiecinski, A. D. Martin, and P. J. Sutton, Phys. Rev. D **47**, 3775 (1993).
[55] K. Golec-Biernat and A. M. Stasto, Phys. Rev. D **80**, 014006 (2009).
[56] G. Watt, A. D. Martin, and M. G. Ryskin, Eur. Phys. J. C **31**, 73 (2003).
[57] S. Catani, M. Ciafaloni, and F. Hautmann, Phys. Lett. B **242**, 97 (1990).
[58] S. Catani, M. Ciafaloni, and F. Hautmann, Nucl. Phys. **B366**, 135 (1991).
[59] J. C. Collins and R. K. Ellis, Nucl. Phys. **B360** 3 (1991).
[60] E. M. Levin, M. G. Ryskin, Yu. M. Shabelski, and A. G. Shuvaev, Sov. J. Nucl. Phys. **54**, 867 (1991).
[61] J. Kwiecinski, A. D. Martin, and A. M. Stasto, Acta Phys. Pol. B **28**, 2577 (1997).